The insulating-to-superconducting transition in europium high-temperature superconducting ceramics

1997 J. Phys.: Condens. Matter 9 901

(http://iopscience.iop.org/0953-8984/9/4/010)

J. Phys.: Condens. Matter **9** (1997) 901–912. Printed in the UK PII: S0953-8984(97)73888-8

The insulating-to-superconducting transition in europium high-temperature superconducting ceramics

Ralph Rosenbaum† and Jan Genossar‡

† Tel Aviv University, School of Physics and Astronomy, Raymond and Beverly Sackler Faculty of Exact Sciences, Ramat Aviv, Tel Aviv 69978, Israel

‡ Technion, Physics Department and Crown Centre for Superconductivity, Haifa 32000, Israel

Received 23 April 1996, in final form 6 September 1996

Abstract. Experiment resistivity data on high-temperature superconducting ceramics of fully oxygenated $EuBa_2Cu_{3-x}Co_xO_y$ show that the insulating-to-superconducting transitions take place at liquid-helium temperature, provided that the cobalt fraction x exceeds 0.3. The resistivity follows a simple power-law dependence $\rho \propto T^{-1/2}$, attributed to electron–electron interactions. A model based upon intrinsic Josephson tunnelling junctions is suggested to explain the transition from insulating to superconducting states.

1. Introduction

At liquid-^{3}He temperature, a number of 3D systems exhibit transitions from the insulating phase to the metallic normal-state phase (IM) as the metallic content of the system is increased. By further increasing the metallic content, a second transition is observed from the metallic state to the superconducting state (MS). Such behaviour has been observed in amorphous Nb_xSi_{1-x} films [1], in amorphous Au_xSi_{1-x} films [2], in amorphous Mo_xGe_{1-x} alloys [3] and recently in 'random' Al–Ge films [4].

In contrast with the IM-to-MS phase diagrams, there have been only a few reports of direct insulating-to-superconducting (IS) transitions, without the presence of an intermediate normal-state metallic phase. One of the first IS transitions was reported by Shapira and Deutscher [5] in granular Al–Al_2O_3 films. Since the temperature range over which activated hopping was observed was limited, one can question whether their temperature fitting range was sufficiently large to confirm the *exponential* behaviour of the resistivity [5]. A convincing explanation for the IS transition was given in terms of a Josephson junction model, in which superconducting Al grains were separated by resistive Al_2O_3 barriers [5].

There has appeared in the literature a great amount of high-quality resistivity data on high-temperature superconductors (HTSCs). Many groups have observed out-of-plane resistivities that increase with decreasing temperature below 100 K, prior to the samples becoming superconducting in the liquid-helium temperature region. Some groups claim that the rising resistivity results from semiconductor behaviour (also referred to as activated hopping, variable-range hopping (VRH), Mott hopping, Efros–Shklovskii hopping or non-metallic behaviour). A few groups claim that the rises in ρ result from quantum corrections to the metallic conductivity from weak localization and/or electron–electron interaction (EEI) (or correlation) effects. Still another large group simply gives no explanation for the rising resistivities. To our knowledge, no HTSC group has used the technique described

0953-8984/97/040901+12$19.50

in section 2 to differentiate between metallic and insulating behaviours. This technique is often used by the metallic-to-insulating (MI) transition community to distinguish between the two behaviours. Once the behaviour has been characterized as metallic or insulating, then the appropriate theories can be fitted to the experimental data.

Many experimentalists try to fit their out-of-plane HTSC resistivity data to the form $\rho_c = aT + b + f(T)$ where the term $aT + b$ describes the high-T metallic behaviour often observed above 100 K. A variety of theoretical expressions for $f(T)$ have been proposed. Anderson and Zou [6] suggested that $f(T) = c/T^1$ based upon a resonating-valence-bond (RVB) theory. Their model involves two types of soliton excitation in the CuO_2 layers. Electrons can tunnel between the layers but then must break up into these excitations. Clearly the $\rho_c \propto c/T$ expression diverges as $T \to 0$. Yan *et al* [7] have suggested the simple activated expression for $f(T)$, namely $f(T) = (c/T)\exp(\Delta/k_BT)$; they suggested that a gap Δ may originate from singlet-pair formation between electrons on opposite planes of a bilayer. Using a model of coherent interplanar tunnelling between neighbouring layers blocked by repeated intraplanar incoherent scatterings, Kumar and Jayannavar [8] predicted that $f(T) \propto T^{-2z}$ where z is small and of the order of unity. Moreover, they found that $\rho_c \propto \rho_{ab}$. In contrast, Radtke and Levin [9], using a model which describes Josephson coupling in terms of incoherent quasiparticle hopping along the c axis, suggested that $f(T) = 1/[d + c(T_0/T)/\sinh^2(T_0/T)]$; for small T_0, their expression reduces to the simple form $f(T) = T_1/(T_2+T)$. As $T \to 0$, $f(T) \to T_1/T_2$. Hence the resistivity is finite and their expression describes metallic behaviour [9]. A publication relevant to our results is that by Wang *et al* [10] who suggested that the MI transition is caused by the effects of both disorder in the lattice and *electron correlations*. The observed maximum in the resistivity followed by the transition to superconductivity at lower temperatures arises from the dominating contribution of superconducting fluctuations. There are two contributions to the superconducting fluctuations: one from the Aslamasov–Larkin process and one from the Maki–Thompson process. Ioffe *et al* have discussed the Aslamasov–Larkin term in connection with HTSCs [11]. The Maki–Thompson process is discussed in [12] and [13].

We list a few relevant and representative experimental publications illustrating the increasing resistivities in HTSCs:

(a) in sintered ceramic pellets of $RBa_2Cu_{3-x}Co_xO_{7-\delta}$, refer to Fisher *et al* [14];

(b) in many different types of polycrystalline sample (ceramics), see Narozhnyi and co-workers [15];

(c) in single crystals of $YBa_2Cu_3O_{7-\delta}$ (YBCO), see Brawner *et al* [16], Ito *et al* [17], Takenaka *et al* [18] and Yan *et al* [7];

(d) in single crystals of $Bi_2Sr_2CuO_y$, refer to Martin *et al* [19], Hou *et al* [20] and Wang *et al* [21];

(e) in single crystals of $Bi_2Sr_2CaCu_2O_{8+\delta}$ (BSCCO), refer to Martin *et al* [22] and Yan *et al* [7];

(f) in Bi–Sr–La–Cu–O crystals, see Jin *et al* [23].

Ando *et al* [24] have recently reported an IS transition in undoped $La_{1.87}Sr_{0.13}CuO_4$. This group used pulsed magnetic fields up to 61 T to quench the superconductivity and found that the normal-state resistivity followed a $\rho(T) \propto \ln(T_0/T)$ dependence which clearly diverges to infinity as $T \to 0$ [24]. This result is in direct conflict with the result of Cieplak *et al* [25] using similar material. Another inconsistency is present in the $La_{1.85}Sr_{0.15}CuO_4$ data with a Zn content of 4% reported by Fukuzumi *et al* [26]. These workers claim an IS transition, in contrast with the claim of Cieplak *et al* that the transition is a MS transition [25]. These disagreements illustrate the general problem of trying to determine whether

the non-superconducting phase is either insulating or metallic. Different sample preparation techniques, limited normal-state data, incorrect analysis methods and biased interpretations can all contribute to the contrasting different claims and inconsistencies concerning the MS transitions in the cuprates.

2. Low-temperature conductivity data and the metallic-to-insulating transition

Thick films and bulk samples may be classified as being either insulating or metallic. Metallic films always display a finite resistivity or a non-zero positive conductivity at absolute zero in temperature. In contrast, insulating films are defined as exhibiting infinite resistivity (zero conductivity) at absolute zero. The criterion that is often used incorrectly to characterize 3D films as *insulating* is that $\mathrm{d}\rho/\mathrm{d}T$ is *negative*. Quantum corrections to the *metallic* conductivity that include weak localization and EEI effects will produce a resistivity that will *increase* with decreasing temperature. Likewise, *activated hopping* processes will lead to an *increasing* resistivity with decreasing temperature. The following procedure allows one to differentiate between metallic and insulating behaviours in films whose resistivities increase with decreasing temperature.

Strongly insulating 3D films exhibit an activated hopping conductivity which can be described by the VRH expression

$$\sigma(T) = \sigma_0 \exp[-(T_0/T)^y] \tag{1}$$

where σ_0 is the pre-factor, T_0 is a characteristic temperature and y is an exponent. For Mott hopping, $y = \frac{1}{4}$ and, for Efros–Shklovskii hopping, $y = \frac{1}{2}$.

In contrast, the conductivity of a 3D metallic film at sufficiently low temperatures can be described by the power-law expression

$$\sigma(T) = \sigma(0) + CT^z \tag{2}$$

where $\sigma(0)$ is the finite zero-temperature conductivity, C is the pre-factor and z is the exponent of the temperature power law. Equation (2) might approximate the conductivity contributions from the 3D EEI theory and/or from the 3D weak localization theory. Note that, in the above procedures, y and z are free fitting parameters. Refer to the review articles of Lee and Ramakrishnan [25] and of Bergmann [26] for introductions to these theories.

A useful technique to identify the MI transition was previously introduced in [29, 30]. The mathematical function $w(T)$ exhibits distinctively different temperature behaviours for insulating and metallic films:

$$w(T) = \mathrm{d}\ln\sigma/\mathrm{d}\ln T = (T/\sigma)\,\mathrm{d}\sigma/\mathrm{d}T. \tag{3}$$

In practice, the w-values are calculated from two conductivity points $\sigma_1(T_1)$ and $\sigma_2(T_2)$ at two close temperatures T_1 and T_2 using one of the following expressions:

$$w(T_{ave}) \approx (\ln\sigma_1 - \ln\sigma_2)/(\ln T_1 - \ln T_2) \tag{4a}$$

or from the approximation

$$w(T_{ave}) \approx T_{ave}(\ln\sigma_1 - \ln\sigma_2)/(T_1 - T_2) \tag{4b}$$

where

$$T_{ave} = (T_1 + T_2)/2.$$

For *strongly insulating* films exhibiting VRH conductivity, inserting equation (1) into equation (3) yields

$$w(T) = y(T_0/T)^y. \tag{5}$$

Note that $w(T)$ increases to *infinity* as the temperature approaches absolute zero. By making a linear-regression fit of the $\log[w(T)]$ versus $\log T$ data, one can directly extract values for the hopping exponent y and for the characteristic temperature T_0 using equation (5). The slope of the linear-regression fit is equal to y, and the intercept I of the fit, is related to T_0 via the expression $T_0 = (10^I/y)^{I/y}$.

For *3D metallic* films exhibiting slowly decreasing conductivities with decreasing temperature, equation (2) can be substituted into equation (3) to yield

$$w(T) = zCT^z/[\sigma(0) + CT^z] = zCT^z/\sigma(T). \tag{6}$$

Observe that, if the film is indeed *metallic* and exhibits a finite positive conductivity $\sigma(0)$ at absolute zero, then $w(T)$ should *extrapolate to zero* at absolute zero. For this case, a linear-regression fit of the $\log(w\sigma)$ versus $\log T$ data yields values for the exponent z and the pre-factor C using equation (6). The slope of the linear-regression fit is equal to the exponent z, and the intercept I of the fit is related to the pre-factor C via the expression $C = 10^I/z$. Values for $\sigma(0)$ follow directly for the different films. Extrapolation of $\sigma(0)$ to zero as a function of metal content x will yield a good estimation for the critical metallic content x_c at the MI transition [30].

Samples might also exhibit *temperature-independent* values for w. Such a temperature-independent behaviour of w can be realized if $\sigma(0)$ is set to zero in equation (2). For this case, the film is insulating, since $\sigma(T) \to 0$ as $T \to 0$ K. Moreover, the low-temperature conductivity data can be fitted very well using the simple temperature power-law expression

$$\sigma(T) = CT^z \tag{7}$$

where C and $z = w$ are the two fitting parameters. Note that a VRH law *cannot* be fitted to conductivity data that exhibit values for w that are *temperature independent*. We refer to samples having conductivities described by equation (7) as 'weakly insulating' samples. Note that, if the VRB theory is valid in HTSCs [6], then $z = w = 1$.

If the conductivity displays a maximum or minimum in temperature, then w will be zero. If the conductivity increases with decreasing temperature showing highly metallic behaviour, e.g. owing to the presence of superconducting fluctuations or to strong spin-orbit scattering, then w becomes negative.

In summary, observing whether w extrapolates to zero or whether w diverges to infinity (and/or remains finite) as $T \to 0$ K will differentiate between metallic and insulating behaviours.

3. Sample preparation and measurement details

Cobalt was chosen as the site-selective dopant, since stoichiometric $RBa_2Cu_{3-x}Co_xO_y$ samples (R = rare earth = Eu or Y) are readily formed under standard synthesis conditions [31]. Europium ceramics should have similar electronic properties to those of YBCO since the ionic radius of Eu^{3+} is very close to the average of the ionic radii of Y^{3+} and Pr^{3+} [14]. The experimental results observed by Fisher *et al* [14] on the resistivity and thermopower of YBCO and of $EuBa_2Cu_3O_{7-\delta}$ (EBCO) ceramics are very similar. Sample preparation has been described in [32, 33]. Sintered pellets or ceramics of fully oxygenated $EuBa_2Cu_{3-x}Co_xO_y$ exhibited good reproducibility of their electronic transport properties from batch to batch and good long-term chemical stability.

The MI transition can be introduced into the $RBa_2Cu_3O_{7-\delta}$ family in several ways: by oxygen depletion, by substitution of Eu by Pr, or by substitution of Cu by trivalent

ions such as Co or Ga and by a combination. Suppression of superconductivity and the crossing of the MI transition is obtained conveniently by substitution of Cu(1) by Co in $YBa_2Cu_{3-x}Co_xO_{7-\delta}$ and in $EuBa_2Cu_{3-x}Co_xO_{7-\delta}$. According to Tarascon *et al* [29], the Co substitutes and occupies the Cu(1) sites in the CuO chains running along the *b* axis in the CuO layer. This substitution should result in the weakening of the coupling between CuO_2 planes in the *c* direction. The cobalt concentrations are nominal and are known with an uncertainty of $\pm 2\%$ in x. As x increased from 0.1 to 0.4, the oxygen content $y = 7 - \delta$ increased from 6.97 to 7.02.

Samples were in the form of rectangular bars or van der Pauw discs. Electrical contacts were made using gold wires that were embedded prior to sintering. Four-terminal resistance measurements were employed. The samples were measured in a standard ^{4}He cryostat, where helium exchange gas provided good thermal contact between the samples and the thermometer. Joule heating was not a problem in these measurements. A few ceramics were measured in a ^{3}He refrigerator. Both the ^{3}He refrigerator and the ^{4}He cryostat were equipped with 4 T superconducting magnets, used to quench the superconductivity partially.

One should be aware that the experiments on ceramic and polycrystalline samples yield only averages over orientations of an assembly of anisotropic crystallites [14, 15]. Our results can be contrasted to the anisotropy ratios of the out-of-plane to in-plane resistivities for YBCO single crystals where Brawner *et al* [16] reported ratios of $\rho_c/\rho_{ab} = 2000$, Ito *et al* [17] observed ratios between 60 and 1700, and Takenaka *et al* [16] found ratios ranging from 60 to 3000. Interestingly, both the magnitudes and the temperature dependences of our measured ceramic resistivities are very similar to the out-of-plane resistivities ρ_c observed for single crystals of YBCO [16–18]. Thus, it appears that the grain boundaries between our sintered crystallites do not play an important role in the overall resistivity values.

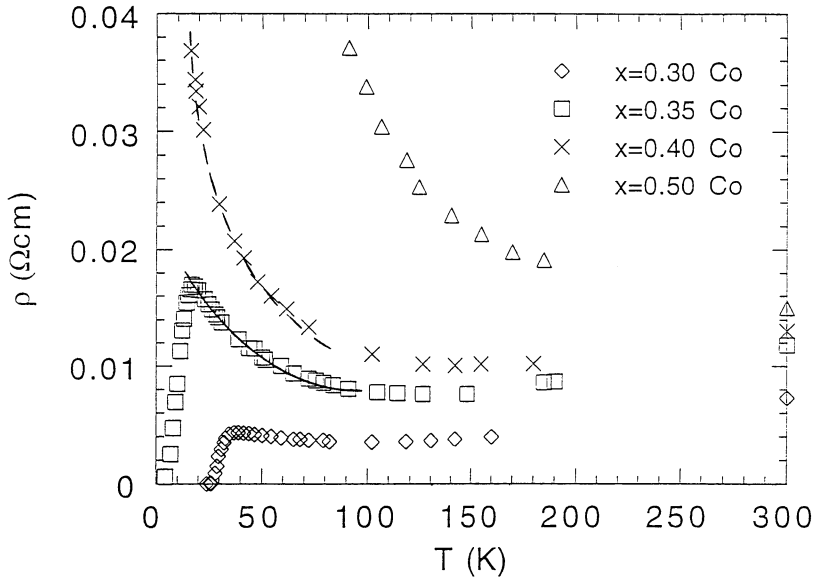

Figure 1. Resistivity versus temperature for sintered ceramics of $EuBa_2Cu_{3-x}Co_xO_y$ ($6.97 \leqslant y \leqslant 7.03$) having different cobalt concentrations x. The lines are fits using the expression $\rho(T) = \sigma^{-1}(T) = (CT^z)^{-1}$ for weakly insulating samples.

4. Experimental results and interpretation

Figure 1 shows the resistivity versus temperature of fully oxygenated sintered pellets of $EuBa_2Cu_{3-x}Co_xO_y$ for different Co contents. It is common practice to display HTCS transport data as resistivity rather than conductivity; thus, we now refer to resistivity rather than to conductivity. For cobalt fractions slightly greater than $x = 0.30$ (30 at.%), the resistivities decrease linearly with increasing temperature between 300 to 150 K and exhibit minima at round 125 K. The interesting region is below 80 K where the resistivity increases rapidly with decreasing temperature. Pellets having Co contents $x = 0.40$ and 0.50 have no superconducting transitions. A detailed study of pellets containing lower Co contents ($x < 0.3$) can be found in [14], where the resistivities decrease over the entire temperature range, and the superconducting transition temperatures occur in the liquid-nitrogen temperature regime. We assume that, if the superconductivity could be quenched in these pellets having $x < 0.3$ with a sufficiently high magnetic field, then these samples would exhibit metallic properties in the normal state.

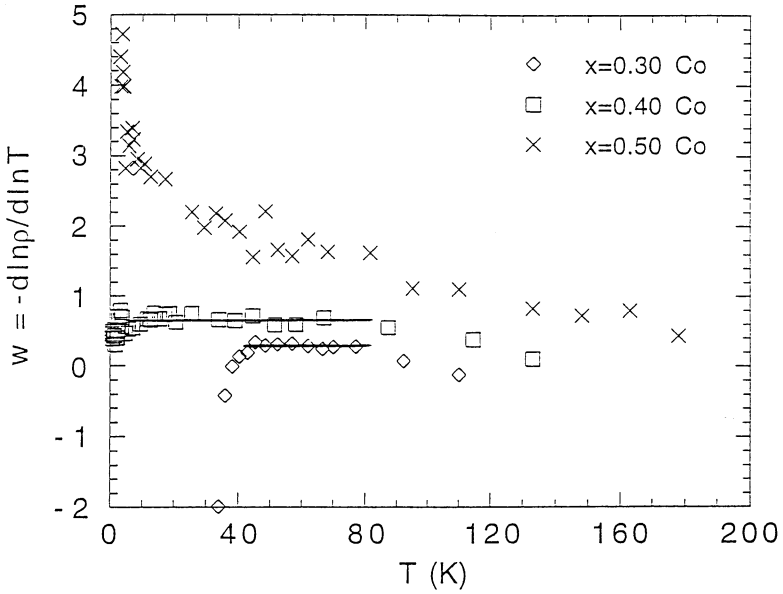

Figure 2. Experimental values of $w(T) = -\mathrm{d}\ln\rho/\mathrm{d}\ln T = \mathrm{d}\ln\sigma/\mathrm{d}\ln T$ versus temperature for sintered ceramic pellets having different cobalt concentrations. If $w(T)$ diverges to infinity as $T \to 0$, as for the case of the $x = 0.50$ cobalt pellet, then the resistivity can be described by the VRH law. Within the temperature range where $w(T)$ is *temperature independent*, as seen for the $x = 0.40$ and 0.30 pellets, the resistivities can be described using the expression $\rho(T) = \sigma^{-1}(T) = (CT^z)^{-1}$ for weakly insulating samples where $z = w$.

For the pellets having a Co content $x \geqslant 0.3$, the w-values are plotted in figures 2 and 3.

For the $x = 0.50$ sample, the w-values clearly diverge in figure 2 as $T \to 0$, and this sample is insulating. There are no signatures of superconductivity. A linear-regression fit of the $\log w$ versus $\log T$ data yields a Mott VRH fit to the resistivity data: $\rho(T) = \rho_0 \exp(T_{Mott}/T)^y$ with $y = 0.26 \pm 0.01$, $T_0 = T_{Mott} = 89\,000 \pm 2000$ K, and $\rho_0 = 8.4 \times 10^{-5} \pm 0.5 \times 10^{-5}$ Ω cm. The fit, shown by the solid line in figure 4, is good in the range 3 K$\leqslant T \leqslant$ 124 K. For the Mott hopping model to be valid, the hopping distance

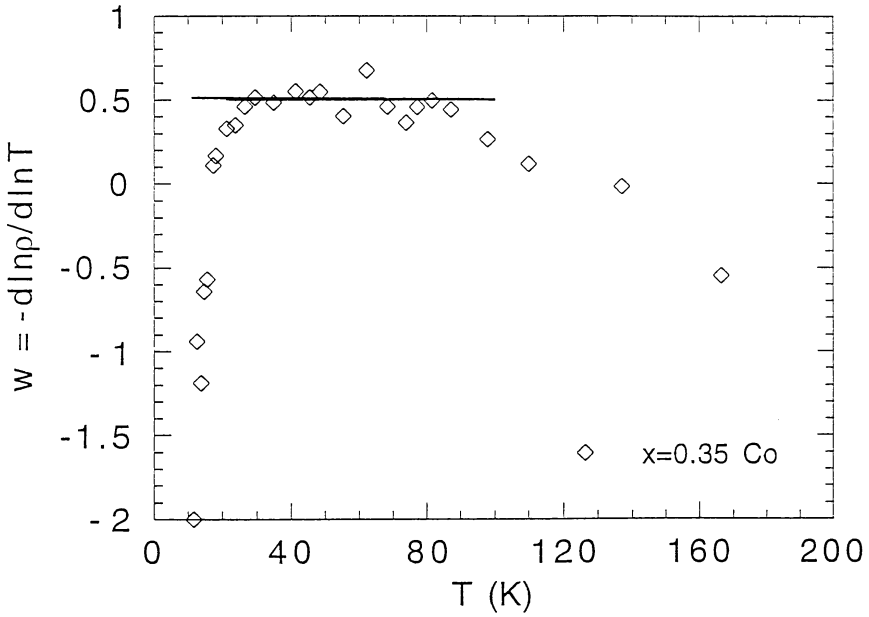

Figure 3. Experimental values of $w(T)$ versus temperature for the $x = 0.35$ cobalt pellet. This sample becomes superconducting at 4 K. Yet in the temperature interval between 80 and 26 K, $w(T)$ is *temperature independent*, implying that the resistivity follows the expression $\rho(T) = \sigma^{-1}(T) = (CT^z)^{-1}$ for an insulator with $w = z = 0.52$.

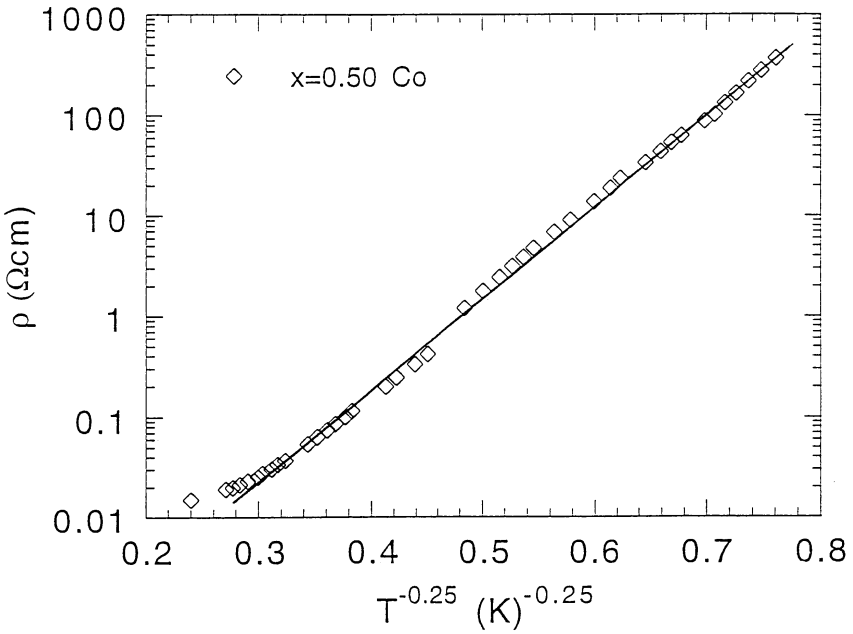

Figure 4. Logarithm of the resistivity versus $T^{-1/4}$ for the $x = 0.50$ cobalt pellet. The resistivity can be described well by a Mott VRH law, as shown by the solid line.

R_{hop} must be equal or greater than the localization length ξ [34]:

$$R_{hop}/\xi = (\tfrac{3}{8})(T_{Mott}/T)^{0.25} \geqslant 1. \tag{8}$$

Recall that the electron is unlocalized and essentially free if R_{hop} is less than the localization length ξ; if $R_{hop} < \xi$, then the sample is metallic in behaviour and the Mott model does not apply. The criterion of equation (8) is satisfied up to the highest temperature of 124 K.

The $x = 0.40$ cobalt sample exhibits a resistivity minimum at 140 K, followed by increasing resistivity down to 0.4 K; there are no indications of superconductivity. Over the wide temperature interval from 72.5 to 6.45 K, w has an approximately constant value of 0.67 as seen in figure 2, and the resistivity data can be fitted well using the expression $\rho(T) = \sigma^{-1}(T) = (CT^z)^{-1} = (4.34T^{0.67})^{-1}$ Ω cm, shown by the broken line in figure 1. In the liquid-^{3}He temperature region, the expression $\rho(T) = \sigma^{-1}(T) = (CT^z)^{-1} = (4.98T^{0.42})^{-1}$ Ω cm gives an acceptable fit. Neither an exponential fit nor a $\rho(T) \propto \ln(T_0/T)$ fit were satisfactory.

In both the $x = 0.5$ and the $x = 0.4$ pellets, there was no superconductivity. We speculate that, owing to the high Co doping level, not only are Cu(1) ions replaced by Co in the CuO chains but that some of the Cu(2) ions in the CuO_2 planes are replaced by Co, thus destroying superconductivity in the CuO_2 planes.

The surprising result comes from the interpretation of the data for the $x = 0.35$ Co pellet from figure 1. This sample exhibits a minimum in its resistivity at 125 K, an increasing resistivity below 100 K, superconducting fluctuations below 24 K, a maximum in its resistivity at 16.5 K and a transition to zero resistivity at 4 K. As seen in figure 3, its w-values are temperature independent between 80 and 26 K; clearly, in this temperature region, this sample exhibits insulating behaviour with the resistivity following a $\rho(T) = \sigma^{-1}(T) = (CT^z)^{-1} = (13.7T^{0.49})^{-1}$ Ω cm dependence as illustrated by the solid line in figure 1. A VRH exponential expression cannot be fitted satisfactorily to this data. This weakly insulating behaviour has recently been observed in two other systems [35, 36]. Martin *et al* [19] also observed $\rho_c \propto T^{-z}$ with $z = 0.61$ for non-superconductor and $z = 0.52$ for superconductor Bi–Sr–Cu–O crystals.

The $x = 0.30$ cobalt pellet exhibits similar behaviour with a resistivity minimum at 102 K, followed by a resistivity maximum at 39 K; superconducting fluctuations are already present at 44 K and the zero-resistivity superconducting state occurs at 24 K. In the temperature region between 77 K to 45 K, w is again temperature independent as seen in figure 2. Although this temperature interval is very limited, there is no suggestion that w will extrapolate to zero at $T = 0$ K; hence this sample appears to be insulating in the normal state. Again, the resistivity data can be fitted using the expression $\rho(T) = \sigma^{-1}(T) = (CT^z)^{-1} = (79.6T^{0.287})^{-1}$ Ω cm.

Application of a 4 T magnetic field partially suppressed the superconducting fluctuation region in the $x = 0.30$ and 0.35 pellets and extended the normal-state region approximately 5 K lower than in the absence of the field as seen in figure 5. Much larger fields must be used in order to quench the superconductivity and to extend the normal state to much lower temperatures. However, the present data give definitive support for an IS transition. In an earlier publication, these data were misinterpreted by the first of the present authors to include the intermediate metallic region [37].

The $T^{-1/2}$ power-law dependence of the resistivity does not agree with any of the theoretical predictions mentioned above. Our results can be explained simply in terms of the EEI theory of Altshuler and Aronov [38]; they predicted that the dominant interaction correction to the conductivity in semiconductors arises in the particle–hole channel or diffusion channel involving interactions between electrons with a small relative momentum.

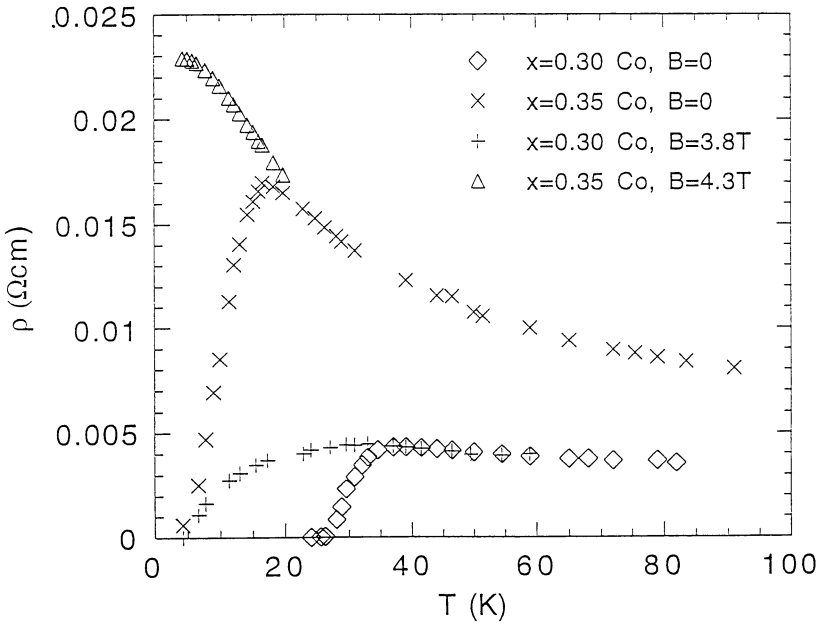

Figure 5. Resistivity versus temperature in the presence of a magnetic field; the applied field depresses the superconducting transitions to lower temperatures. Fields much greater than 4 T must be used in order to extend the normal-state phase to much lower temperatures for the purpose of analysing the weakly insulating regime.

The conductivity correction is given by

$$\sigma_{EEI}(T) = \frac{1.294}{\sqrt{2}} \frac{e^2}{4\pi^2 \hbar} \left(\frac{4}{3} - \frac{3}{2} \tilde{F}_\sigma \right) \left(\frac{k_B T}{\hbar D_{dif}} \right)^{1/2} \tag{9}$$

where the electron screening parameter $\tilde{F}_\sigma$ ranges between 0.2 and 0.4 for many metallic films. Note that the $T^{1/2}$ dependence is in close agreement with the temperature power term observed in these ceramics. If one chooses a typical D_{dif}-value of 0.25×10^{-4} m^2 s^{-1}, then the pre-factor C takes the value of 4 Ω^{-1} cm^{-1} K$^{-1/2}$, close to the experimental values. The electron screening parameter is related to the carrier concentration n; however, the effective mass of the carrier and the relative dielectric constant of the HTSC must be known to evaluate n [27]. It is thought that the EEI expression in equation (9) also applies if the carriers are *holes* instead of *electrons* [39]. We speculate that the EEI process is a global intrinsic process that is not restricted to any particular plane in the crystalline structure of the HTSC. The $T^{1/2}$ conductivity correction of the 3D EEI theory should be contrasted to the 2D EEI prediction that $\sigma_{EEI} = C \ln T$ [27, 38]. If the conductivity were to be solely confined to the CuO_2 planes, one would anticipate an insulating $\ln T$ dependence.

A possible explanation for the IS transition was suggested by Shapira and Deutscher [5] and Deutscher *et al* [40] for granular Al_2–Al_2O_3. We expand their model. Al grains are coated with an insulating shell of Al_2O_3. We shall assume that the barriers exhibit a weakly insulating behaviour in their resistivity. The Al grains become superconducting at some temperature T_c. Above T_c the resistance of the granular material can be modelled as two resistors *in series*, namely one resistor representing the metallic resistivity behaviour of

all the grains and the second resistor representing the insulating resistivity behaviour of all the barriers. Below room temperature, the metallic grain resistor decreases in magnitude while the barrier resistor increases. At these temperatures the barrier resistor is smaller than the grain resistor; hence the grain resistor dominates, producing the decrease in resistance. Near liquid-helium temperature, the barrier resistor begins to dominate and produces the overall increase in the resistance. The grains will exhibit superconducting fluctuations above the transition temperature T_c and then become superconducting at T_c. Josephson tunnelling junctions are now formed, consisting of two superconducting grains separated by an insulating barrier between them. As the temperature is further decreased below T_c, the thermal energy $E_T(T) = k_B T$ is reduced proportionally. Provided that the barrier resistance $R_N(T)$ is not too high and the temperature is sufficiently low, the Josephson coupling energy $E_J(T)$ can exceed the thermal energy. At this temperature, the Josephson junction will short out this section of the film. Other junctions, having slightly higher normal-state resistances, will become superconducting at slightly lower temperatures. Eventually, the entire sample exhibits zero resistivity at a sufficiently low temperature. The Josephson coupling energy is given by the Ambegaokar–Baratoff [41] expression

$$E_J(T) = [\pi h/4e^2 R_N(T)]\Delta(T)\tanh[\Delta(T)/2k_B T] \tag{10}$$

where $\Delta(T)$ is the temperature-dependent energy gap and $R_N(T)$ is the normal-state resistance of the junction, namely the barrier resistance between the two grains. Thus, this explanation assumes the presence of superconducting grains or crystallites separated by insulating barriers.

Can the Deutscher *et al* model be applied to YBCO and EBCO? The YBCO structure consists of CuO_2 planes separated by other atomic layers along the *c*-axis direction. Numerous theories have been proposed that the high-T_c superconductivity originates in these 2D CuO_2 atomic planes. It is believed that the CuO_2 bilayers couple together by the Josephson currents along the *c*-axis direction. After the pioneering experiment of Kleiner *et al* where intrinsic Josephson junctions were observed in single crystals of BSCCO [42], intrinsic Josephson junctions have recently been observed in YBCO by Chen's group [43], by Tonouchi *et al* [44] and by Rapp *et al* [45]. Thus, if we interchange the Al grains with the CuO_2 planes, and if we replace the Al_2O_3 barriers by other non-superconducting planes (such as the BaO, CuO and Eu planes), then the above argument for the IS transition should still be valid.

A completely different explanation might possibly be based upon a charge-density-wave (CDW)-driven structural phase transition [46–48]. However, HTSCs do not have the 1D wire structure required for CDW phenomena.

Acknowledgments

We are much obliged to Professor B Fisher and Dr L Patlagan of the Technion for the sample preparation. We acknowledge Professor T Fujita of Hiroshima University for directing us to the relevant references. We thank Dr Guenter Fuchs and Dr Arnulf Möbius of the IFW for informative discussions and Rachel Rosenbaum for editing assistance. The Tel Aviv University group acknowledges financial support from the German–Israeli Foundation and the Internal Research Fund of Tel Aviv University. The Technion group acknowledges funding from the Israel Science Foundation administered by the Israel Academy of Sciences and Humanities and by the Fund for the Promotion of Research at the Technion.

References

[1] Herte G, Bishop D J, Spencer E G, Rowell J M and Dynes R C 1983 *Phys. Rev. Lett.* **50** 743
[2] Furubayashi T, Nishida N, Yamaguchi M, Morigaki K and Ishimoto H 1985 *Solid State Commun.* **55** 513
[3] Yoshizumi S, Mael D, Geballe T H and Greene R L 1985 *Localization and Metal–Insulator Transitions* ed H Fritzsche and D Adler (New York: Plenum) p 77
[4] Shoshany J, Goldner V, Rosenbaum R, Witcomb M, McLachlan D S, Palevski A, Karpovski M, Gladkikh A and Lereah J 1996 *J. Phys.: Condens. Matter* **8** 1729
[5] Shapira Y and Deutscher G 1983 *Phys. Rev.* B **27** 4463
[6] Anderson P W and Zou Z 1988 *Phys. Rev. Lett.* **60** 132
[7] Yan Y F, Matl P, Harris J M and Ong N P 1995 *Phys. Rev.* B **52** R751
[8] Kumar N and Jayannavar A M 1992 *Phys. Rev.* B **45** 5001
[9] Radtke R J and Levin K 1995 *Physica* C **250** 282
[10] Wang N L, Ruan K Q, Pan G Q, Chen Z J and Cao L Z 1995 *J. Phys.: Condens. Matter* **7** 4875
[11] Ioffe L B, Larkin A I, Varlamov A A and Yu L 1993 *Phys. Rev.* B **47** 8936
[12] Aronov A G, Hikami S and Larkin A I 1989 *Phys. Rev. Lett.* **62** 965
[13] Bieri J B and Maki K 1990 *Phys. Rev.* B **42** 4854
[14] Fisher B, Genossar J, Patlagan L, Reisner G M and Knizhnik A 1996 *J. Appl. Phys.* **80** 898
[15] Narozhnyi V N, Kochetkov V N, Khlybov E P and Alekseevskii N E 1994 *Fiz. Met. Metalloved.* **78** 75 (Engl. Transl. 1994 *Phys. Met. Metallogr.* **78** 173)
Narozhnyi V N and Kochetkov V N 1995 *Phys. Rev.* B **53** 5856
[16] Brawner D A, Wang Z Z and Ong N P 1989 *Phys. Rev.* B **40** 9329
[17] Ito T, Takagi H, Ishibashi S, Ido T and Uchida S 1991 *Nature* **350** 596
[18] Takenaka K, Mizuhashi K, Takagi H and Uchida S 1994 *Physica* C **235–240** 1339
[19] Martin S, Fiory A T, Fleming R M, Schneemeyer L F and Waszczak J V 1990 *Phys. Rev.* B **41** 846
[20] Hou, X H, Zhu W J, Li J Q, Li J W, Xiong J W, Wu F, Huang Y Z and Zhao Z X 1994 *Phys. Rev.* B **50** 496
[21] Wang N L, Geibel C and Steglich F 1996 *Physica* C **260** 305
[22] Martin S, Fiory A T, Fleming R M, Espinosa G P and Cooper A S 1989 *Appl. Phys. Lett.* **54** 72
[23] Jin R, Ott H R and Grindatto D P 1995 *Physica* C **250** 395
[24] Ando Y, Boebinger G S, Passner A, Kimura T and Kishio K 1995 *Phys. Rev. Lett.* **75** 4662
[25] Cieplak M Z, Guha S, Kojima H, Lindenfeld P, Xiao G, Xiao J Q and Chien C L 1992 *Phys. Rev.* B **46** 5536
[26] Fukuzumi Y, Mizuhashi K, Takenaka K and Uchida S 1996 *Phys. Rev. Lett.* **76** 684
[27] Lee P A and Ramakrishnan T V 1985 *Rev. Mod. Phys.* **57** 308
[28] Bergmann G 1984 *Phys. Rep.* **107** 1
[29] Möbius A 1989 *Phys. Rev.* B **40** 4194
[30] Rosenbaum R L, Slutzky M, Möbius A and McLachlan D S 1994 *J. Phys.: Condens. Matter* **6** 7977
[31] Tarascon J M, Bardoux P, Miceli P F, Greene L H, Hull G W, Eibschutz M and Sunshine S A 1988 *Phys. Rev.* B **37** 7458
[32] Fisher B, Genossar J, Patlagan L and Reisner G M 1993 *Phys. Rev.* B **48** 6056
[33] Fisher B, Genossar J, Patlagan L and Reisner G M 1994 *Phys. Rev.* B **50** 4118
[34] Castner T G 1990 *Hopping Transport in Solids* ed M Pollak and B I Shklovskii (Amsterdam: North-Holland) p 1
[35] Friedman J R, Zhang Y, Dai P and Sarachik M P 1996 *Phys. Rev.* B **53** 9528
[36] Rosenbaum R, Heines A and Pilosof M 1996 Preprint
[37] Rosenbaum R, Shoshany J, Fisher B, Genossar J and Patlagan L 1995 *Hopping and Related Phenomena* ed O Millo and Z Ovadyahu (Jerusalem: The Hebrew University, Racah Institute of Physics) p 175
[38] Altshuler B L and Aronov A G 1983 *Solid State Commun.* **46** 429
Altshuler B L and Aronov A G 1985 *Electron–Electron Interactions in Disordered Systems* ed A L Efros and M Pollak (Amsterdam: North Holland) p 1
[39] Bergmann G 1996 private communication
[40] Deutscher G, Entin-Wohlman O, Fishman S and Shapira Y 1980 *Phys. Rev.* B **21** 5041
[41] Ambegaokar V and Baratoff A 1963 *Phys. Rev. Lett.* **10** 486 (Errata 1963 *Phys. Rev. Lett.* **11** 104)
[42] Kleiner R, Steinmeyer F, Kunkel G and Muller P 1992 *Phys. Rev. Lett.* **68** 2394
[43] Ling D C, Yong G, Chen J T and Wenger L E 1995 *Phys. Rev. Lett.* **75** 2011
[44] Tonouchi M, Itoh A, Yasuda T, Shimakage H, Wang Z and Takano S 1996 *Czech. J. Phys.* **46** suppl. S3, 1275

[45] Rapp M, Murk A, Semerad R and Prusseit W 1996 *Phys. Rev. Lett.* **77** 928
[46] Greenblatt M, McCarroll W H, Neifeld R, Croft M and Waszczak J V 1984 *Solid State Commun.* **51** 671
[47] Matsuda Y, Sato M, Onoda M and Nakao K 1986 *J. Phys. C: Solid State Phys.* **19** 6039
[48] Thorne R E 1996 *Phys. Today* **49** 42